Ordered Structures of Poly(*p*-hydroxybenzoic acid). 2. Low-Energy Chain-Packing Structures

Natalia V. Lukasheva

Institute of Macromolecular Compounds of the Academy of Science of Russia, Bolshoi pr. 31, St. Petersburg 199 004, Russia

Thomas Mosell,† Alla Sariban,† and Jürgen Brickmann*,†,‡

Institut für Physikalische Chemie I and Darmstädter Zentrum für Wissenschaftliches Rechnen, Technische Hochschule Darmstadt, Petersenstrasse 20, D-64287 Darmstadt, Germany

Received February 22, 1995; Revised Manuscript Received November 6, 1995⊗

ABSTRACT: A detailed analysis of the packing of polymer chains of *p*-hydroxybenzoic acid in the low- and high-temperature range is presented. Chain conformations and the orientation of the chains in the unit cell have been determined by a molecular mechanics approach, based on a two-step procedure consisting of grid-scan calculations and a Monte-Carlo-type study. Intramolecular and intermolecular degrees of freedom were considered simultaneously in the optimization process. The low-temperature structures of polymer samples (phases I and II) were found to be more stable than the structures observed in oligomer samples. In phase I, the cell parameters that are perpendicular to the chain axis tend to be smaller in the calculations than in experiments. Furthermore, the calculations suggest the existence of polymorphism at a microscopic level due to the coexistence of several packing possibilities with comparable stabilities.

I. Introduction

The crystalline modifications of the aromatic polyester poly(*p*-hydroxybenzoic acid) (PHBA) have extensively been studied in experiments.[1−9] Four crystalline modifications have been described so far. Two of them (referred to as phases I and II in this paper) are stable at room temperature. Additionally, two high-temperature modifications (phases III and IV) have been observed. The information about the crystal cells is summarized in Table 1, which also contains transition temperatures and the kind of disorder observed in these phases.

It was concluded from experimental data[3,5,6,8] that the changes during the structure transitions take place mainly in layers of phenyl rings that are perpendicular to the chain axis. In a preceding paper[10] (hereafter referred to as paper I) we presented the results of calculations about the intermolecular interactions in such layers. The main features of PHBA chain-packing and the possible motions of chain fragments were analyzed for phases I to IV. The calculations revealed a possibility for orientational rearrangements of chain fragments consisting of a phenyl ring and two neighboring ester groups in phases III and IV.

In this work, PHBA chain-packing is considered in more detail. The atomistic modeling approach has been extended: Intramolecular interactions are now taken into account. The cell parameters are included as additional degrees of freedom. Both parallel and antiparallel arrangements of neighboring chains are considered.

A straightforward scanning of the accessible part of configurational space, as performed in paper I,[10] is impossible due to the increase in the number of degrees of freedom. In the present work, a two-step procedure is used to elucidate the details of the PHBA structures. In the first step, only a few degrees of freedom are considered in a grid-scan procedure applied to identify the regions of configurational space that correspond to local minima of the packing energy. Consecutively, the structure parameters obtained by the grid-scan procedure are used as the starting point of a Monte-Carlo (MC) type scanning of the vicinity of the minima. The chain conformations and the orientation of the chains relative to the unit cell are determined for all experimentally observed structures of PHBA.

This paper is organized as follows. The model and the simulation method are described in section II. Section III contains the results from the grid-scan calculations, and the results obtained from the MC-type study are presented in section IV. In section V, some conclusions are drawn.

II. Model and Method

(A) Polymer Chain and Crystal Structure. The two-monomer repeat unit of the PHBA polymer chain is depicted in Figure 1. Torsion τ_1 describes the rotation of the chain around a virtual bond formed by the substituents of the phenylene moiety. The dihedral angle τ_1 is determined from atoms of two successive ester groups ($C_7-O-C_{14}-O_3$). The dihedral angle τ_3 is defined by the torsion $C_4-C_7-O-C_8$. The corresponding dihedral angles for the second monomer of the repeat unit are denoted by τ_2 and τ_4, respectively. The helical structure of the chain is determined by the values of these four dihedral angles. Another dihedral angles is necessary to represent the rotation angle of the phenyl-ring plane with respect to an ester group. The dihedral angle τ_5 (τ_6 for the other phenyl ring) is defined by the torsion $C_7-O_1-C_8-C_9$. Note that τ_5 and τ_6 only influence the phenyl ring and have no effect on the chain backbone.

The values of the valence angles $\nu_1-\nu_3$ of the main chain change significantly during the rotation of a phenyl ring.[11] Therefore, the energy values obtained

* To whom correspondence should be addressed.
† Institut für Physikalische Chemie I.
‡ Darmstädter Zentrum für Wissenschaftliches Rechnen.
⊗ Abstract published in *Advance ACS Abstracts,* January 15, 1996.

0024-9297/96/2229-1286$12.00/0

Table 1. Main Features of the Crystal Modifications of PHBA[a]

cryst modification	temp (°C)	cell params (Å)			type of cryst cell	type of disorder	refs
		a	*b*	*c*			
phase I	≤325	7.47−7.62	5.67−5.72	12.4−12.62	orthorhombic	defects	1−3
phase II (oligomer)	≤260	3.77−3.78	11.06−11.1	12.8−12.89	orthorhombic	defects	1, 4
phase II (polymer)	≤260	3.67	10.64	12.6	orthorhombic	defects	for *a*, *b*: 1 for *c*: 4
phase III	360−430	9.13−9.24	5.28−5.35	12.49−12.5	pseudohexagonal	reorientational	1, 3, 5−8
phase IV	440 to degradation	9.35	5.4	12.45−12.46	hexagonal	rotational	3, 9

[a] The intermediate temperatures correspond to transition regions.

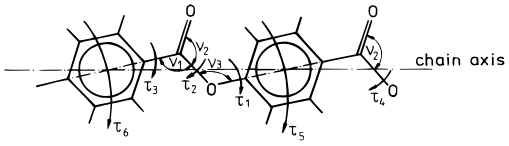

Figure 1. Dihedral angles $\tau_1-\tau_6$ and valence angles $\nu_1-\nu_3$ of the two-monomer repeat unit of the PHBA chain. The *trans* configuration displayed in this figure corresponds to $\tau_1 = \tau_2 = 180°$.

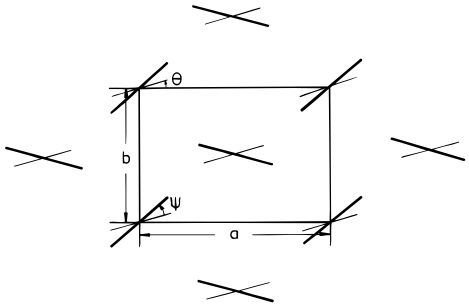

Figure 2. Schematic view of a plane that is orthogonal to the chain axis. The setting angle θ is defined as the angle between the crystallographic plane $a-c$ and the plane of symmetry of the chain. The angle Ψ between the phenyl ring and the plane of symmetry results from the dihedral angles $\tau_1-\tau_6$.

in the calculations may be improved considerably by adjusting the valence angles to the requirements of the intramolecular conformation. The valence angles $\nu_1-\nu_3$ were varied as a function of the dihedral angles τ_5 and τ_6 in a way described in part C of this section. All other valence angles and the bond lengths were kept fixed. Thus, phenyl rings are treated as rigid.

Some external parameters, whose variation may strongly influence the energy of a structure, are also considered in this work. The cell parameters *a* and *b* must be taken into account, because a change in these parameters affects the nonbonded interactions between atoms of neighboring chains. Conversely, cell parameter *c* is not treated as an independent variable, because the axis *c* is parallel to the chain axis of PHBA, and accordingly, *c* can be determined from the intramolecular conformation of the chain.

A further degree of freedom is the setting angle θ that describes the angle between the coordinate system of the chain and the coordinate system of the unit cell (see Figure 2). The setting angle is defined as the angle between the plane of the first ester group (the left end of the chain, when it is placed as in Figure 1) and the crystallographic plane $a-c$. In paper I, the setting angle had been defined as the angle between the crystallographic plane $a-c$ and the plane of the ester groups. This definition is no longer appreciable, because the consideration of the dihedral angles $\tau_1-\tau_6$ as degrees of freedom allows the chains to adopt helical conformations without a plane of symmetry.

The high densities of the solid-state modifications of PHBA can only be obtained with chain conformations of a highly extended character, as has already been shown for polymers with similar geometries.[12] Therefore, in the first step only flat conformations have to be considered. On this basis, conformations with *trans* and *cis* orientation of successive ester groups, i.e. rod-like and crankshaft-like chains, are used in the grid-scan calculations.

Helical superstructures are considered in the MC-type calculations. The transformation of the atomic coordinates to the reference frame of the helix was performed according to the approach of Miyazawa and Sugeta[13,14] for ordinary spirals. The use of a helix representation for the chains will only be appropriate if the length of one turn of the spiral is not very large. The displacements from a straight rod will otherwise be insignificant for a finite chain segment, and the helix axis can be approximated by the major axis of the radius-of-gyration tensor.[12]

The potential-energy calculations of the multichain crystal structure was performed for chain segments that consisted of six monomer units at the grid-scan stage and of 10−14 monomer units in the MC-type calculations. The main features of the structures can be determined by considering the dominant contributions to the packing energy. Therefore, only the intermolecular interactions of a reference chain segment with the shell of its nearest-neighbor chains were taken into account at the grid-scan stage, while interactions between the reference chain segment and three shells of surrounding chains were considered in the MC-type calculations.

(B) Determination of the Low-Energy Structures. The calculation procedure consists of a two-step approach. The two steps differ not only in the number of degrees of freedom considered at each stage but also in the method applied in the search for the energy minima.

In the first step, a grid for a small number of essential degrees of freedom was used in a straightforward scanning of configurational space similar to the approach of paper I.[10] Only the dihedral angles τ_5 and τ_6 for the rotation of the phenyl rings and the setting angle θ were considered in these calculations. The values of these angles were varied in steps of 10°. This choice for the variables restricts the configurational space to flat *trans* and *cis* conformations, i.e. the conformations with the highest packing densities. The dependence of the valence angles $\nu_1-\nu_3$ on the dihedral angles was taken into account in the grid-scan calculations. Values averaged from the experimental data were used for the unit cell parameters *a* and *b*. Cell parameter *c* results from the length of the repeat unit and, therefore, depends slightly on the values of the valence angles.

In the second step, structures that were obtained in step one were used as starting configurations for a random search of the parameter space in the vicinity of these structures. For phases I and II, all grid-scan structures within 1.5 kcal/mol of the structure with the

lowest energy were used as starting configurations. The structures within 2.5 kcal/mol were used for phases III and IV. The variables in this MC type procedure included the dihedral angles $\tau_1-\tau_6$, the cell parameters a and b, and the setting angle θ. In each MC trial, new values for all nine parameters were chosen randomly. Deviations from the minimum-energy configurations of the grid-scan calculations up to ±10° for the angles (±30° in the high-temperature modifications) and ±1.0 Å for the cell parameters were allowed in the calculations. The deepest (local) energy minimum was determined from a total of at least 10^6 MC trials for every starting structure. Additionally, the structure with the lowest energy was determined for each 10^3 trials. These structures were examined to get an impression of the possible fluctuations of the parameters in structures that are only slightly less favorable than the minimum. We are convinced that the number of iterations is sufficiently large to obtain structures that contain all the characteristics of the true minimum-energy structure.

(C) Force Field. An all-atom force field is used for the energetic representation of the PHBA polymer. The interaction energy E consists of contributions from torsional potentials V_τ and from the intermolecular interactions V_{INTER} between the atoms of a reference chain segment and the atoms of the chains contained in the appropriate number of shells:

$$E = \sum_{\mathrm{i}} V_\tau(\tau_{\mathrm{i}}) + V_{\mathrm{INTER}} \qquad (1)$$

All energy values reported in this paper are stated for one two-monomer repeat unit.

The difficulties that were encountered in the determination of torsional potentials for aromatic polyesters have been extensively discussed in numerous papers.[15−18] The heights of the rotational barriers of the ester group depend strongly on the computational approach that is applied to the problem.[17a,19] The proper shape of the rotational potential can be obtained from semiempirical AM1[20] calculations,[17a] but the rotational heights are usually underestimated by this method.[21] Coussens *et al.*[19] obtained a scaling factor of 1.9 to correct the rotational barriers of torsions that are in conjugation to aromatic rings. Experimental results for the gas-phase barrier could be reproduced within an accuracy of 15% by applying this scaling factor. Moreover, the barrier heights are in good agreement with the results of *ab initio* calculations on phenylbenzoate performed by Jaffe *et al.*[18]

The scaling factor for the rotational barriers has already been used in the parameterization of a force field for aromatic polyesters.[11] This force field was based on AM1 calculations of the dimer of *p*-hydroxybenzoic acid in vacuum. The rotational barriers for the dihedral angles τ_5 and τ_6 correspond to the joint rotational barriers of torsions E and G of the parameterization. However, a major part of the intramolecular degrees of freedom that were taken into account by the parameterization are frozen in the present work. This can significantly affect the rotational barriers of the ester-group torsions.[22] Therefore, the torsional parameters of the parameterization may not be transferred to the present calculations. Instead of creating a new set of parameters, we used the scaled AM1 potential-energy values as obtained from the calculations in vacuum. Thus, all intramolecular forces are included in the torsional potentials. Additional AM1 calculations were performed for this work to reduce the difference between the dihedral angles of two successive conformations to 5°. A cubic spline was used for the interpolation between two energy values.

Table 2. Changes of the Main-Chain Valence Angles as a Function of Dihedral Angles τ_5 and τ_6 in the AM1 Geometries

	valence angle (deg)		
dihedral angle τ_5 or τ_6 (deg)	ν_1	ν_2	ν_3
0	112.1	120.2	124.4
90	113.2	118.1	118.5

The values of the main-chain valence angles $\nu_1-\nu_3$ were adjusted as a function of the dihedral angles τ_5 and τ_6. The valence angles for the dihedral angles 0 and 90° were taken from the optimized AM1 geometries. The data are listed in Table 2. A linear interpolation was used for intermediate angles in the calculations.

The dihedral angles τ_3 and τ_4 correspond to torsion F of ref 11. No torsional potential was applied to these dihedral angles although the rotational barrier for torsion F is the highest among the three ester-group torsions. This simplification is justified as long as the dihedral angles τ_3 and τ_4 of the low-energy structures are in the vicinity of the minimum of torsion F. The applicability of this approach to the PHBA structures will be discussed further down.

The intermolecular interactions between atoms in different chains were calculated by the potential function:

$$V_{ij}(r_{ij}) = A\mathrm{e}^{-Cr_{ij}} - Br_{ij}^{-6} + \frac{1}{4\pi\epsilon_0\epsilon_{\mathrm{r}}}\frac{q_i q_j}{r_{ij}} \qquad (2)$$

The dispersive interactions were calculated with the parameter set of Dashevskij[23] (for a list of the parameters see also Table 1 for paper I[10]). The point charges for the Coulomb interactions were taken from ref 11. They had been obtained from a Mulliken population analysis of the AM1 results.

The electrostatic interactions were calculated with a distance-dependent dielectric constant ϵ_r. The approximation of Block and Walker[24] was used for the representation of short- and long-range Coulomb interactions. At distances shorter than a crossover distance $d^* = 3.3$ Å, the dielectric constant is taken to be unity, while a bulk value for the dielectric constant (taken to be $\epsilon_{\mathrm{BULK}} = 3.5$ in our calculations) is approached asymptotically for large distances:

$$\epsilon_r = \epsilon_{\mathrm{BULK}}^{(1-r^*/r_{ij})} \quad \text{for} \quad r_{ij} > 1.1r^* \qquad (3)$$

A fifth-order polynomial is used for interatomic distances $r^* < r_{ij} < 1.1\ r^*$ to join the two parts of the function smoothly. The same dependence on the intermolecular distance was applied by Rutledge and Suter[12] in their calculations of crystalline structures of polyaramids.

III. Results of the Grid-Scan Calculations

In this section, the results of grid-scan calculations are reported and discussed. Packing energies were determined for flat crankshaft-like conformations of the main chain with the phenyl-ring rotation angles as variables. A summary of the results of listed in Table 3. The values marked by asterisks refer to structures that have been used as initial structures for the MC calculations reported in section IV.

Table 3. Results of the Grid-Scan Calculations

chain conformation	phase	dihedral angle τ_5 (deg)	dihedral angle τ_6 (deg)	setting angle θ	arrangement of chains	type of packing[a]	lowest energy for structure[b] (kcal/mol)
cis	phase I	30 (150)	30 (150)	90	parallel	bc	−21.68
	phase I	30 (150)	30 (150)	90	antiparallel	bc	−25.72*
trans	phase I	30 (150)	30 (150)	90	parallel	bc	−24.48*
	phase II	30 (150)	30 (150)	0	parallel	bc	−24.46*
	phase II	30 (150)	30 (150)	0	parallel	sc	−25.75*
	phase II	30 (150)	30 (150)	0	antiparallel	sc	−25.98*
cis	phase III	30	20	0	antiparallel	bc	−22.77*
	phase IV	30	30	0	antiparallel	bc	−22.68*

[a] Types of packing: bc = body-centered, sc = side-centered. [b] Values indicated by asterisks refer to structures that were chosen as initial structures for the MC-type calculations.

(A) Phase I. Grid-scan calculations with the cell parameters of phase I were performed for body-centered cells with a *cis* conformation of the chain. The energetically most favorable configurations were obtained for a setting angle of $\theta = 90°$. Here, the results for this setting angle are presented, though calculations were performed for different setting angles with a spacing of 10°.

An important question in the context of chain-packing is the preference of a parallel or antiparallel arrangement of the polymer chains in the crystal cell. This question has not been finally resolved so far. Lieser[1] had proposed space group $P2_12_12_1$ for phase I, suggesting an antiparallel arrangement of neighboring chains. However, X-ray diffraction measurements could not distinguish between a packing with parallel and with antiparallel polarity of neighboring chains, because the data revealed no sensitivity to chain polarity.[25]

The lowest energy in the grid-scan calculations for a structure with antiparallel chain-packing is around 4 kcal/mol lower than that for parallel chain-packing. The differencs mainly result from the electrostatic interactions between ester groups of neighboring chains. These interactions are significantly more favorable for an antiparallel orientation of the chains.

The contour maps for the dependence of the packing energy on the rotation angles τ_5 and τ_6 of the phenyl rings in phase I are displayed in Figure 3a,b for, respectively, parallel and antiparallel chain packing. In both maps, the lowest energy has been chosen as the zero-point of the energy scale. In the region around these minima, each line indicates an increase in packing energy of 1 kcal/mol. Regions with energies higher than 8 kcal/mol are displayed as white areas.

A comparison of the two maps reveals no significant differences, either in the location of the minima or in the energy differences relative to the minima of the maps. Both contour maps contain two pairs of the symmetrical minima; the minima at $\tau_5 = 30°$, $\tau_6 = 30°$ and at $\tau_5 = 150°$, $\tau_6 = 150°$ correspond to an orientation of successive phenyl rings in the same direction, while the minima at $\tau_5 = 30°$, $\tau_6 = 150°$ and $\tau_5 = 150°$, $\tau_6 = 30°$ correspond to an opposite orientation of successive phenyl rings. The latter minima are ca. 0.5 kcal/mol higher in energy than the former. This difference can be attributed to the electrostatic interactions between phenyl rings with similar and opposite rotation angles in neighboring chains.

The rotational freedom of the chain fragments is, therefore, similar in both structures, and the criterion of energy is sufficient for the evaluation of the stability of the structures. As a result, the question of parallel or antiparallel arrangement of chains can be resolved in favor of an antiparallel arrangement. This antiparallel arrangement of the chains is the only structure of phase I that was selected as the initial configuration for the MC-type calculations.

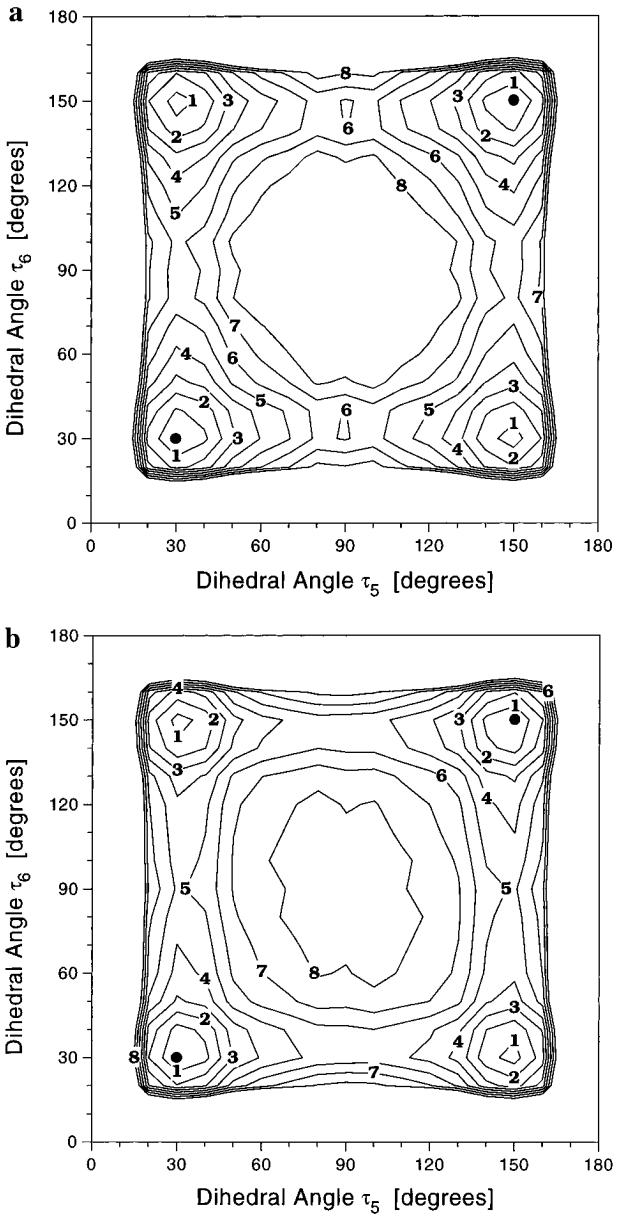

Figure 3. Contour maps (in kcal/mol) for the dependence of the packing energy on the rotation angles τ_5 and τ_6 in phase I. The results for (a) parallel and (b) antiparallel arrangements of the chains were both determined with the grid-scan procedure with a setting angle $\theta = 90°$. Energies are given relative to the lowest energy for each structure, and the zero-point of the energy scale does not give any indication of the absolute value of the minimum energy.

The grid-scan results described so far were obtained with fixed values for the cell parameters that were averaged from the experimental data. Additional cal-

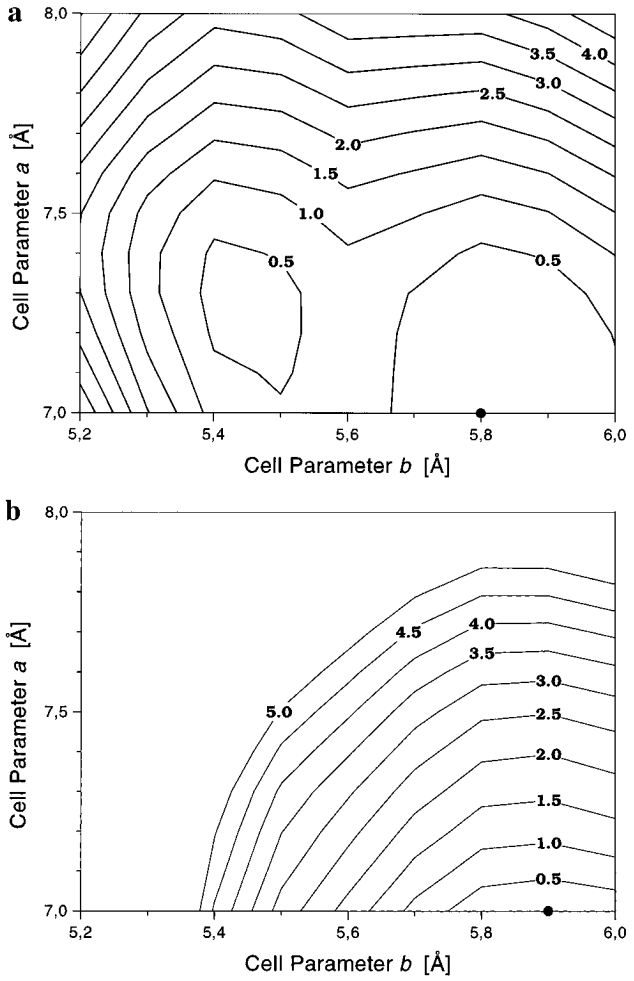

Figure 4. Contour maps (in kcal/mol) for the dependence of the packing energy on the cell parameters *a* and *b* in phase I. The contour maps were calculated for an antiparallel arrangement of chains at a setting angle $\theta = 90°$. The dihedral angles of τ_5 and τ_6 are (a) both 25° and (b) both 30°. Energies are given relative to the lowest energy for each structure, and the zero-point of the energy scale does not give any indication of the absolute value of the minimum energy.

culations were performed for phase I in order to examine the dependence of the packing energy on the cell parameters. These calculations were performed for the dihedral angles in the chain conformation with the lowest energy ($\tau_5 = \tau_6 = 30°$) and for angles nearby.

The contour maps for the dependence of the packing energy on the cell parameters *a* and *b* are displayed in Figure 4a,b for phenyl-ring rotation angles $\tau_5 = \tau_6 = 30°$ and $\tau_5 = \tau_6 = 25°$, respectively. Again, the zero-point of each pilot indicates the lowest energy for this structure. The conformation with phenyl-ring rotation angles $\tau_5 = \tau_6 = 25°$ is 1.3 kcal/mol more favorable than the chain conformation with $\tau_5 = \tau_6 = 30°$. In comparison to the results for the calculations with the experimental cell parameters, the values of τ_5 and τ_6 tend to be smaller. In both maps, the values of the cell constants *a* and *b* in the structure with the lowest energy are far from the experimental values. For phase I of PHBA, the decrease of the cell parameters leads to significantly lower energies. The energy minimum of Figure 4b corresponds to −28.49 kcal/mol; i.e. the shrinking of the cell parameters lowers the energies by ca. 2.8 kcal/mol. A similar tendency for calculated cell parameters to be smaller than those experimentally observed was found in a theoretical investigation of one of the crystalline phases of cellulose.[26]

A possible explanation for this deviation from the experimentally observed cell parameters is the strong dependence of experimental structure parameters on the conditions of phase formation. This effect is known to be a major problem in the experimental investigation of crystalline low-temperature modifications of polymers. Crystalline low-energy structures are not reached because of quenching or cooling processes, which are applied to stop the chemical reaction of polymer formation. Significant fluctuations of experimental cell parameters have to be expected and have indeed been reported for the crystalline modifications of PHBA (compare Table 1). For PHBA, more careful cooling processes show a tendency of the cell parameters to become smaller, as the crystals approach thermal equilibrium.[1] It is possible that the formation of a crystal structure with higher densities may be unfavorable in the temperature range of the formation of phase I. At these temperatures, a larger volume of the unit cell may be favored due to nonflat main-chain conformations. Moreover, the application of energy minimization results in the creation of the structures that are most favorable at 0 K, and part of the discrepancies in the cell parameters may be due to a temperature dependence of these parameters. However, the discrepancy between calculated and experimental results occurs mainly for cell parameter *b*, whereas Hanna and Windle[6] observed that the changes in cell parameter *a* are larger than those in parameter *b* in the temperature range from −100 to +450 °C. Therefore, the discrepancy in cell parameter *b* should not simply be attributed to thermal expansion.

(B) Phase II. The crystalline modifications phase II is stable for PHBA chains with a low degree of polymerization. In this work, the chain packing of polymer samples is considered, and the effects of short chains and the influence of the end groups on the chain conformations and the crystal structure of phase II are, therefore, neglected. A detailed analysis of the influence of the packing of the end groups on the configuration of phase II would be a task for a separate investigation.

One significant difference between the crystal structure of phase II and the other crystal structures is the length of cell parameter *c*,[1] i.e. the length of the two-monomer repeat unit of the polymer chain. In oligomer samples of phase II, a value of $c = 12.9$ Å has been found, while in polymer samples with a higher degree of polymerization, and in samples where phases I and II coexist, cell parameters $c \approx 12.6$ Å have been observed. It has been supposed that short chains are forced into an extended form with increased valence angles (up to 120°) due to effects related to the packing of the end groups in the interlamellar regions of the oligomer crystals.[1] The influence of the end groups decreases with increasing chain length, while the polymer gradually adopts a bent conformation.

In our approach, where chain-end effects are not taken into account, a cell parameter *c* of ca. 12.6 Å has to be expected and was, indeed, observed in the grid-scan calculations, where the length of the repeat unit can only be influenced by the valence angles. Stronger deformations of the valence angles resulting from packing requirements of the end groups cannot be taken into account as long as the valence angles are chosen according to optimized AM1 geometries. Therefore, concentrating on a more polymer-like version of the unit cell of phase II is appropriate for our simplified force-field approach.

It has been concluded from experiment that the main chain has a *trans* conformation in phase II.[1] The setting

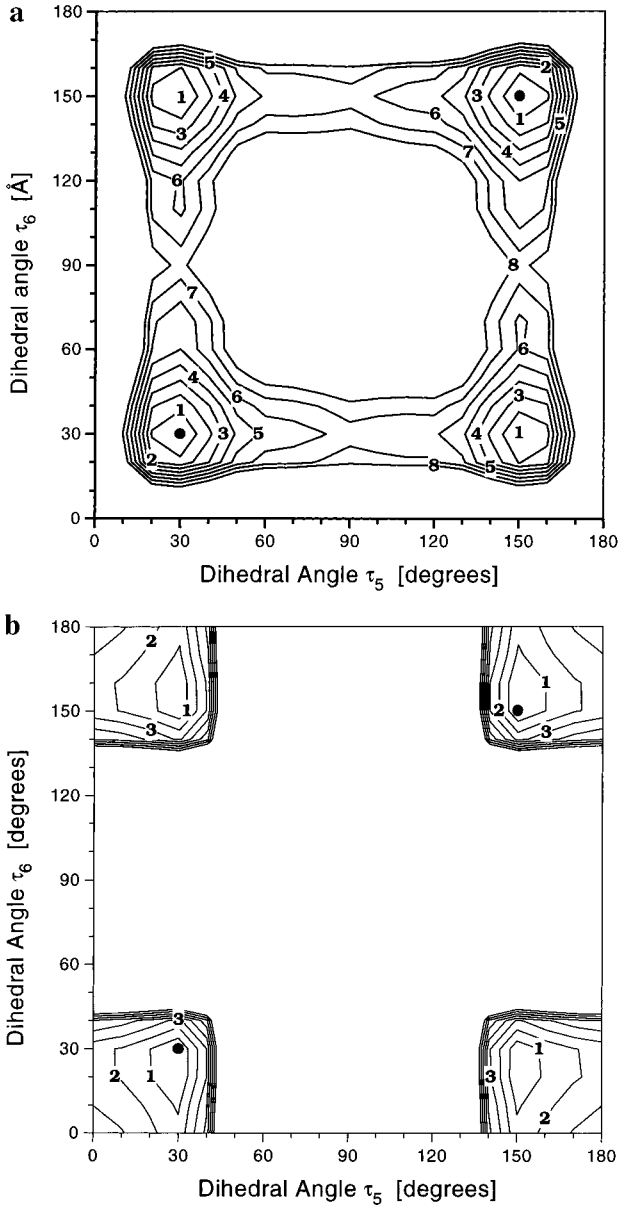

Figure 5. Contour maps (in kcal/mol) for the dependence of the packing energy on the rotation angles τ_5 and τ_6 in phase II. The results have been obtained for side-centered packing of (a) parallel and (b) antiparallel arrangements of the chains. Energies are given relative to the lowest energy for each structure, and the zero-point of the energy scale does not give any indication of the absolute value of the minimum energy.

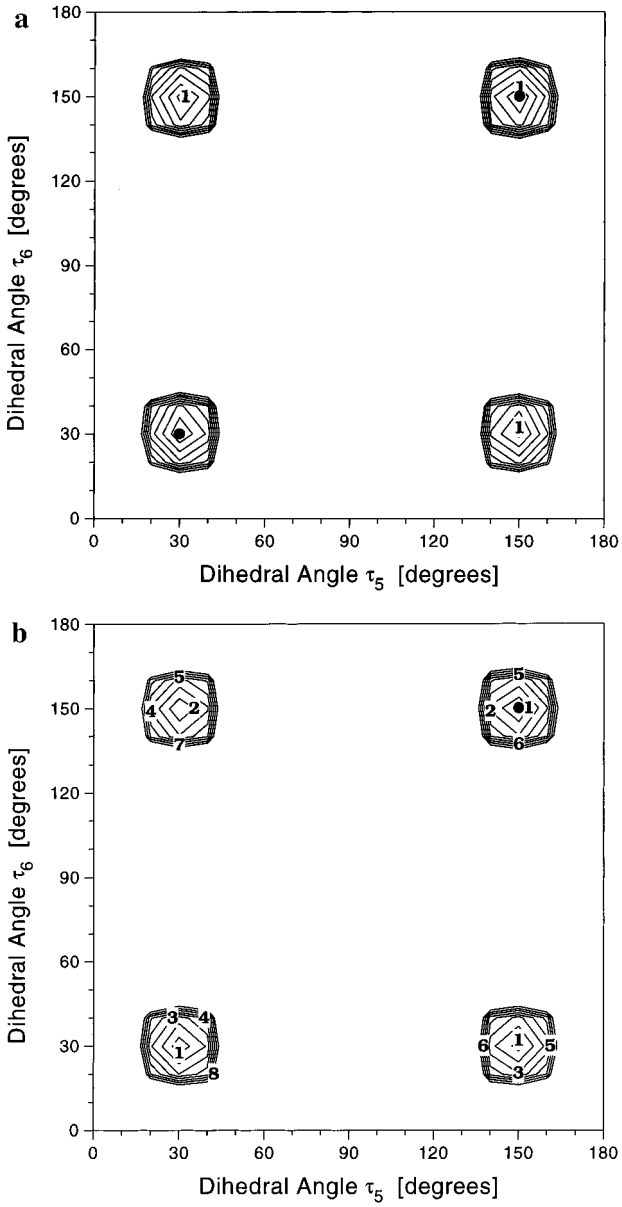

Figure 6. Contour maps (in kcal/mol) for the dependence of the packing energy on the rotation angles τ_5 and τ_6 for a parallel arrangement of chains in a body-centered packing of *trans* conformations. Results are depicted for (a) phase II (setting angle 0°) and (b) a structure with the cell parameters of phase I (setting angle 90°). Energies are given relative to the lowest energy for each structure, and the zero-point of the energy scale does not give any indication of the absolute value of the minimum energy.

angle was fixed to 0° for the grid-scan calculations according to the results presented in paper 1.[10] A unit cell with the cell parameters of phase II can be obtained by packing PHBA chains in a body-centered (0, 0, 0 and $^1/_2$, $^1/_2$, $^1/_2$) or a side-centered (0, 0, 0 and $^1/_2$, $^1/_2$, 0) unit cell. Therefore, both types of unit cell had to be considered in our calculations.

The contour maps for a side-centered packing of the chains in the crystal cell of phase II are displayed in Figure 5a for a parallel and in Figure 5b for an antiparallel arrangement of the chains. The lowest energies of both configurations are close to the lowest energy that was obtained for the most stable structure of phase I with experimental cell parameters. The strong restrictions to the rotational freedom of the phenyl rings in this phase have already been observed in the calculations of paper I.[10] This effect may contribute to the decreased stability of phase II at increased temperatures.

When an antiparallel arrangement of the chains is assumed for a body-centered packing of *trans* conformations, strong steric hindrances are observed and the chains would have to be strongly bent. Therefore, this possibility will not be considered in detail here. Conversely, a parallel arrangement in a body-centered cell is plausible. The results for this type of packing are depicted in Figure 6a. The energy is slightly higher than that for a side-centered packing, but the energy difference to the side-centered structures is relatively small in comparison to the possible decrease in energy due to the inclusion of additional degrees of freedom. Therefore, not only both side-centered structures but also the body-centered structure with a parallel arrangement of the chains has to be considered as an initial structure for the structure refinement in the MC procedure.

The possibility of coexistence for phases I and II over a wide temperature range implies that the differences of the packing energies of these phases are small (at least for chains of an intermediate degree of polymerization) and that the system does not exhibit high energetic interphase boundaries, i.e. chains in a *trans* conformation not only may form crystal cells of phase II but also can participate in chain packing with the crystal cell of phase I.

Therefore, a study of the crystal structure of phase II should consider the relationship of this structure to similar arrangements of the phase I type. The cell parameters of phase II are related to those of phase I by (approximately) a halving of parameter *b* and a doubling of parameter *a*. The contour map for the body-centered packing of *trans* conformations in a parallel arrangement with the experimental cell parameters of phase I has been depicted in Figure 6b. The plane of the main chain, i.e. the plane with the carbonyl groups, lie in the crystallographic plane *b*−*c* instead of the crystallographic plane *a*−*c* that is appropriate for the crystal cell of phase II. The lowest energy is, however, nearly equal to that in the calculation with the parameters of phase II displayed in Figure 6a.

The general features of the contour maps for the *trans* conformation that was obtained with the cell parameters of phase I and for the structure of phase I, i.e. the *cis* conformation depicted in Figure 3, are similar. However, the body-centered cell with parallel arrangement of *trans* chains is about 1.5 kcal/mol less stable than that for the crystal structure of phase I described above.

(C) Phases III and IV. At high temperatures, the thermal fluctuations of the instantaneous values of the dihedral angles increase. The average cross-section of the polymer chain becomes more or less circular, and the packing of the chains in the crystallographic plane *a*−*b* changes to pseudohexagonal in phase III. In comparison to phase I, the unit cell is significantly expanded, mainly due to the increase in cell parameter *a*. The true hexagonal symmetry is finally reached at 435 °C, when phase IV becomes the stable modification.

Grid-scan calculations for phases III and IV have been performed with parallel and antiparallel arrangement of the chains, but structures with very low energies were only obtained for antiparallel chain packing. The contour maps for the crystal cells of phases III and IV with antiparallel arrangement of the chains are displayed in Figure 7a,b respectively. The main features of the PHBA chain packing, the location of the minima and their energy, are similar for phases III and IV. The regions with comparably low energies are wider in the high-temperature phases than in phase I. This provides a larger rotational freedom for the phenyl rings, and the relatively high energies of the low-energy structures can obviously be compensated by entropy contributions.

IV. Results of the Monte-Carlo-Type Calculations

Experimentalists have reported varying results for the cell parameters *a* and *b* of phase I. It was pointed out above that these significant fluctuations of the cell parameters show that the equilibrium structure of phase I is probably not reached in the experimental investigations. For this reason, the cell parameters *a* and *b* were varied in this work within a large range (5.0 Å ≤ *a* ≤ 6.0 Å and 7.0 Å ≤ *b* ≤ 8.0 Å) in order to determine the low-energy structures of phase I by the MC-type calculations.

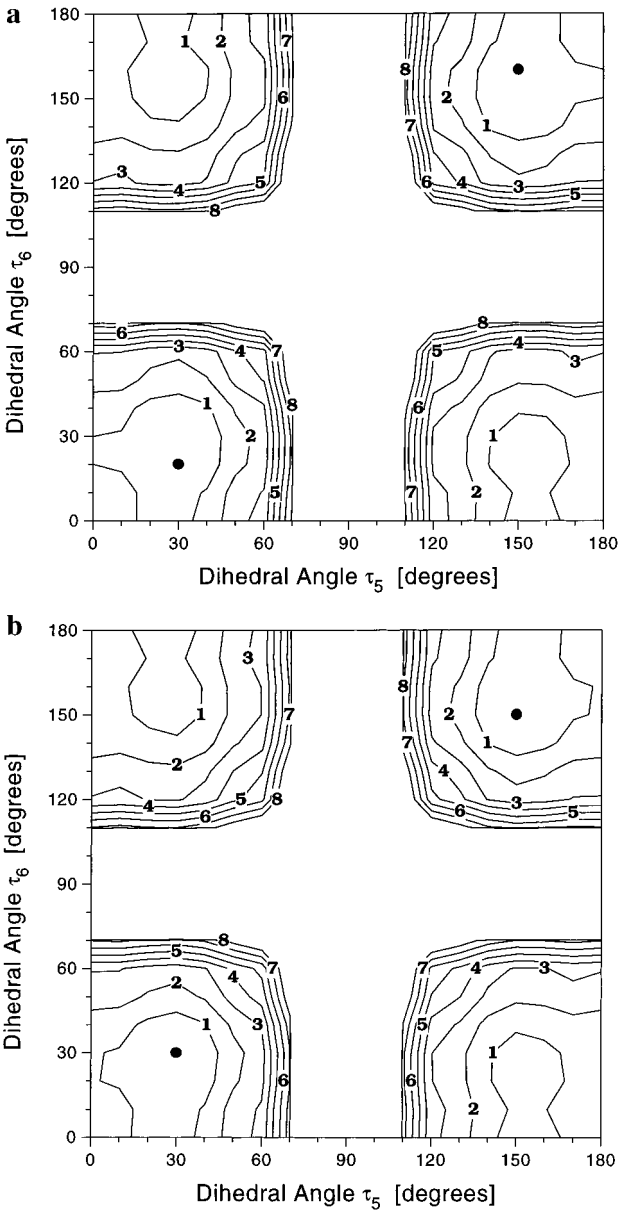

Figure 7. Contour maps (in kcal/mol) for the dependence of the packing energy on the rotation angles τ_5 and τ_6 in phases (a) III and (b) IV with antiparallel arrangement of the chains. Energies are given relative to the lowest energy for each structure, and the zero-point of the energy scale does not give any indication of the absolute value of the minimum energy.

The MC-type calculations result in four different possible structures with very similar values for the cohesive energy. These structures, summarized in Table 4, differ in the values of τ_5 and τ_6 and correspond to the four minima of the contour map in Figure 3b. The cell parameters of all these structures are significantly smaller than those of the experimental structures. Particularly, the cell parameter b = 5.16 Å of the structure with the lowest packing energy is much smaller than the experimental value of 5.67−5.72 Å. The chain conformations of these four structures are close to a flat conformation of the main chain, and therefore, the structures are similar to the corresponding low-energy configurations from the grid-scan calculations. Although the MC calculations confirm the significant tendency toward cell parameters that are smaller than those of the experimental results, the shift of τ_5 and τ_6 toward angles of 25° is not confirmed in the MC results. All values of the phenyl-ring rotation angles are in the vicinity of 30° (or 150°).

Table 4. Results of the MC-Type Calculations for Phase I[a]

dihedral angles (deg)						cell params (Å)				
τ_1	τ_2	τ_3	τ_4	τ_5	τ_6	*a*	*b*	*c*	setting angle θ (deg)	energy (kcal/mol)
9.1	0.5	176.3	177.7	28.1	30.7	7.47	5.16	12.64	93.3	−31.01
−2.5	−0.4	−179.4	179.9	149.9	151.6	7.22	5.30	12.64	87.3	−30.30
−2.5	−3.6	−176.8	−176.5	153.0	29.8	7.34	5.38	12.63	88.1	−29.86
−0.3	4.0	−179.4	−179.8	30.0	153.8	7.18	5.44	12.64	89.8	−29.41
4.0	−1.9	177.1	177.1	28.0	26.7	7.45	5.69	12.64	−91.7	−28.30[b]

[a] Structures with the lowest cohesive energy for local minima. [b] Parameters *a* and *b* varied within the experimental range.

Table 5. Results of the MC-Type Calculations for Phase II[a]

					dihedral angle (deg)						cell params (Å)				
no.[b]	structure info[c]				τ_1	τ_2	τ_3	τ_4	τ_5	τ_6	*a*	*b*	*c*	setting angle θ (deg)	energy (kcal/mol)
1	bc	*t*	p	h	−176.8	−176.2	176.0	−178.6	26.3	28.7	3.78	10.59	12.68	1.7	−28.45
2	bc	*c*	a	h	−0.8	1.6	−175.4	−176.7	30.9	27.5	3.72	10.80	12.63	−2.8	−30.20
3	sc	*t*	p	p	178.7	−178.6	−178.0	177.1	25.9	27.9	3.76	10.51	12.67	−3.0	−29.92
4	sc	*t*	a	p	177.8	177.9	−175.5	−179.9	26.9	32.1	3.80	10.50	12.67	4.5	−30.10
5	sc	*c*	p	p	−4.9	−4.5	−178.0	−179.7	28.1	28.1	3.80	10.49	12.64	−0.4	−27.60
6	sc	*c*	a	p	0.3	−1.5	−177.8	−178.9	25.7	26.0	3.79	10.80	12.64	−4.8	−29.61
7	bc	*t*	p	h	175.0	−176.3	−179.0	178.0	32.7	31.5	3.71	11.08	12.68	5.0	−28.29
8	sc	*t*	a	h	−179.8	178.0	175.1	−175.7	27.2	27.3	3.70	11.01	12.67	−3.3	−27.91
9	sc	*t*	p	h	179.8	178.6	−179.4	179.5	28.3	32.9	3.73	11.01	12.68	−1.2	−27.96

[a] Structures with the lowest cohesive energy for local minima. [b] Structures 1−6: wide range of cell parameters *a* and *b*. Structures 7−9: cell parameters *a* and *b* in the vicinity of the experimental values. [c] First row: bc = body-centered, sc = side-centered. Section row: *c* = *cis*, *t* = *trans*. Third row: a = antiparallel, p = parallel arrangement of chains. Fourth row: h = herringbone, p = parallel packing of phenyl rings.

The comparison between the energies for phase I in Tables 3 and 4 indicates a strong addition stabilization at the level of the MC-type calculations. The inclusion of the interactions between the reference chain segment and the second and third shell of surrounding chains contributes only ca. 2.0 kcal/mol to the energy difference. The remaining stabilization has mainly to be attributed to the change in the cell parameters.

Additional MC-type calculations were performed to investigate possible structures of the samples that are produced by experimental researchers. The cell parameters *a* and *b* were varied in a small range around the experimental values. The structure with the lowest energy (also included in Table 4) is located in the minimum region at $\tau_5 = \tau_6 = 30°$, but similar results were obtained for the other three minima. The cohesive energy of these structures is ca. 3 kcal/mol less favorable than that of the structure of phase I with the lowest energy. Structures with energies within 1 kcal/mol of −28.3 kcal/mol occurred for different variations of cell parameters, indicating the existence of a continuum of structures with parameters that can accept any value within the region of interest. There is no indication of a local minimum that corresponds to a metastable structure. More probably, the structures with the experimental cell parameters are located in a broad region of the energetic hypersurface that descends directly to the global minimum. Phase I can be expected to contain regions with rod-like chains (*trans* conformation of the main chain), because the energy for that structure is close to the packing energy for the structures with the experimental cell parameters. We assume that the great variety of possible structures is the main origin of the spread of the experimental data for the crystal structure of phase I.

According to experimental data[1,4] the cell parameters that are observed for oligomer and polymer samples of phase II are different. The parameters *a*, *b*, and *c* of the polymer crystals are smaller than those of the oligomer crystals (see Table 1). In the MC-type calculations the cell parameters *a* and *b* were varied in a wide range, which included the experimental values for both polymer and oligomer crystals. These calculations were used to determine the cell parameters for the low-energy structures of polymer phase II. Additionally, calculations with the experimental cell parameters of oligomer phase II (variation of *a* and *b* in a small range) were performed to obtain possible low-energy structures for the oligomer phase.

The results of the Monte-Carlo-type calculations for phase II are listed in Table 5. Low-energy structures for phase II were calculated for a body-centered and for a side-centered placement of the chains in the crystal cell. Parallel and antiparallel arrangements of the chains, as well as *trans* and *cis* conformations of the main chain were considered. Table 5 contains structures located in the minimum region near $\tau_5 = \tau_6 = 30°$. Similar results were obtained for the other three minima.

In the low-energy structures obtained with cell parameters *a* and *b* as variables, cell parameter *b* is close to its experimental value in polymer phase II and significantly smaller than in oligomer phase II. Cell parameter *a* is in the vicinity of the experimental value for oligomer crystals, but it is not far from the experimental value of polymer crystals either. The structures with the lowest energies are the body-centered packing of antiparallel chains with *cis* conformation, the side-centered packing of parallel or antiparallel chains with *trans* conformation and the side-centered packing of antiparallel chains with *cis* conformation. The packing energies for these structures are close to those of phase I.

The good agreement between the calculated and the experimental values of the cell parameters implies that the calculated low-energy structures for polymer phase II can be reached in experimental investigations. Crystals of polymer phase II can contain regions with body-centered and with side-centered placement of chains, because of the energy difference between these structures is comparably small. Moreover, the small energy difference between parallel and antiparallel arrangements of chains can lead to some disorder with neighboring chains that are either parallel or antiparallel.

Few structures for oligomer phase II with experimental cell parameters are included in Table 5. Low

energies are only found for *trans* conformations of the main chain, because the chains in the oligomer crystals are strongly stretched. The packing energies for these low-energy structures are higher than those of polymer phase II (by ca. 2 kcal/mol) and those of phase I (by ca. 3 kcal/mol).

The energies for oligomer phase II are comparable to those of two of the possible structures for polymer phase II and to those of the structures for phase I with experimental cell parameters. This result can account for the coexistence of oligomer phase II with phase I and polymeric phase II in some experimental samples[1] that were obtained by heating oligomer samples to temperatures lower than the crystal−liquid crystal transition temperature. These polymer crystals need not consist of the structures with the lowest packing energies. After cooling, these samples should contain regions of phase II with body- and side-centered placement of parallel and antiparallel chains. The main chain must be in a *trans* configuration in the oligomer structures, but can be *cis* as well as *trans* in the polymer structures.

The criterion of energy is practically sufficient for the determination of equilibrium structures in low-temperature crystal phases. By comparison, the determination of chain conformations and cell parameters in ordered high-temperature structures should properly be based on a minimization of the free energy. However, in the framework of the present approach, only structures that correspond to minima of the potential energy can be investigated. The results of these MC-type calculations for the high-temperature phases are presented in Table 6.

In a high-temperature structure, the experimental results for the cell parameters can be considered as characteristic for the equilibrium structures. Therefore, the variation of cell parameters *a* and *b* was limited to the vicinity of the experimental values. Only the parameters that determine the chain conformation have to be optimized. However, at temperatures of 350 and 430 °C, where phases III and IV, respectively, become stable, all structures with cohesive energies within at least 1 kcal/mol of the lowest energy, and not only the structure with the lowest cohesive energy, should reasonably be considered in a discussion of possible equilibrium structures for phases III and IV.

In paper I,[10] the possibility of reorientational motion for crankshaft-like chain fragments was reported for phases III and IV. This reorientational motion consists of a change of the placement of a crankshaft-like chain fragment between the crystallographic planes *a*−*c* and *b*−*c*. A comparison of the low-energy structures with setting angles 0 and 90° reveals a difference in cohesive energy of about 1 kcal/mol (for one monomer) between the two preferable positions for the plane of symmetry of the main chain. This energy difference, which is observed in both phases, is slightly greater than the difference calculated in paper I. The increase has to be attributed to differences in the geometry of the chain between the model of paper I and that of the present work. However, an energy difference of 1 kcal/mol is not of fundamental importance in the temperature range where phases III and IV are stable.

The accessible range of angles for the dihedral angles τ_1, τ_2, τ_5, and τ_6 has approximately doubled in phases III and IV in comparison to phase I. Therefore, there is an increased flexibility in the possible conformations of the main chain and a greater rotational freedom for the phenyl rings in high-temperature phases. The range of the results for the dihedral angles τ_3 and τ_4,

Table 6. Results of the MC-Type Calculations for Phases III and IV

		dihedral angles (deg)						cell params (Å)				
		τ_1	τ_2	τ_3	τ_4	τ_5	τ_6	*a*	*b*	*c*	setting angle θ (deg)	energy (kcal/mol)
III	min[a]	3.3	4.5	−178.8	−178.0	29.4	28.8	9.23	5.24	12.63	0.6	−23.62
	range[b]	−3.8 to +4.9	−5.0 to +5.0	177.6−183.5	177.5−183.2	23.0−33.9	21.4−32.5	9.12−9.23	5.24−5.34	12.62−12.63	−1.6 to +1.8	
III	min	1.9	2.6	−177.5	178.5	28.2	31.8	9.16	5.28	12.62	85.7	−21.90
	range	−4.0 to +4.0	−5.0 to +3.9	178.2−186.3	177.8−183.6	21.6−33.2	23.5−36.2	9.12−9.19	5.26−5.32	12.62−12.63	85.1−89.3	
IV	min	0.8	−4.5	−178.3	−177.5	27.2	27.4	9.35	5.38	12.63	0.3	−23.21
	range	−5.0 to +4.7	−7.8 to +3.6	176.4−184.8	176.7−184.8	23.6−34.2	24.1−34.5	9.32−9.37	5.36−5.42	12.61−12.63	−0.7 to 2.2	
IV	min	5.4	11.2	178.5	173.2	25.5	39.1	9.36	5.38	12.61	81.8	−21.30
	range	−3.5 to +8.7	−2.0 to +11.2	174.8−187.1	171.9−184.6	21.1−33.1	27.5−39.1	9.32−9.37	5.36−5.41	12.61−12.63	80.4−86.1	

[a] min: structures with the lowest cohesive energy for local minima. [b] range: range of values for the different parameters in the structures within 1 kcal/mol of the structure with the lowest energy. For angles around ±180°, negative values are stated as values larger than 180°.

which correspond to a rotation around the central bond of the ester group, widens in the transition from phase III (5−6°) to phase IV (8−12°). In section II, it has already been pointed out that torsional potentials would have to be introduced, if significant deviations from 0° were apparent, because the dihedral angles τ_3 and τ_4 may have a very great influence on the conformation of the main chain. However, the deviations from 0° are negligible in the low-temperature phases, and the relatively small contribution to the cohesive energy of the torsional potential at a dihedral angle around 12° is of minor importance in a high-temperature phase. Therefore, the omission of an additional torsional potential for τ_3 and τ_4 in the calculations was justified.

The dihedral angles τ_3 and τ_4 do not induce a significant turn in the chain. The neglect of these degrees of freedom in the grid-scan calculations was, therefore, justified. Neither do τ_1 and τ_2 contribute significantly to a helical conformation of the chain. All calculated structures possess the common feature of a strong chain extension, and no essential stabilization of the structures is created by the introduction of these dihedral angles as additional degrees of freedom for the MC-type calculation.

The MC-type calculations were used not only to locate the energy minimum but also to get information about different structures in the vicinity of this minimum. In the MC-type calculations of phases I, III, and IV with cell parameters constricted to the experimental range, the packing energies of about 40−50% of the configurations are within 1 kcal/mol of the lowest energy value for each structure. Therefore, the configurations belong to single-minimum regions with small slopes.

V. Conclusions

The possible packing structures for all the crystal phases of PHBA observed in experiments have been investigated by a molecular mechanics approach. Low-energy structures were calculated by a two-step approach that consists of grid-scan calculations and MC-type calculations.

A body-centered structure with an antiparallel arrangement of the chains was found to be the most stable structure for phase I. The cell parameters *a* and *b* of the structures with the lowest energies tend to be smaller than those reported by experimentalists. We suppose that the discrepancy between the calculated and the experimental cell parameters of phase I may be attributed to a preconditioning of the parameters of phase I due to the initial formation of phase II. The cell parameters *a* and *b* of phase I are approximately double and half those of phase II. We assume that the calculated cell parameters of phase I (modified by the inclusion of lattice expansion due to thermal motion) could be obtained in experimental samples, if phase I were produced directly without the intermediate occurrence of phase II. In the range of the experimental cell parameters, a great variety of structures is possible, which explains the difficulties in the experimental determination of the crystal structure of phase I.

The variety of possible structures is even larger for phase II. The chains can be packed in a body-centered as well as in a side-centered cell. Not only an antiparallel but also a parallel arrangement of the chains is possible. The calculated and the experimental cell parameters of polymer phase II are in good agreement, and accordingly, the minimum-energy structure of this phase can be obtained in experimental investigations. While the stability of polymer phase II is comparable to that of phase I, the structures calculated for oligomer phase II are less stable than those possible for phase I. However, the energy of phase I with the experimental cell parameters is as high as the lowest energy for oligomer phase II.

The lowest energies for structures with the cell parameters of phases III and IV were observed for an antiparallel arrangement of the chains. The calculations indicate an increased conformational flexibility for the main chain and a greater rotational freedom for the phenyl rings in the high-temperature phases. A more detailed investigation of these aspects will have to rely on Monte-Carlo calculations.

The molecular mechanics calculations disclosed a very complicated picture of the PHBA structure. A certain amount of polymorphy at the molecular level has to be expected in the structures of all PHBA crystal modifications. We assume that well-defined samples cannot be made under experimental conditions and that the structure should strongly depend on the conditions of the formation of the sample.

Acknowledgment. This work was supported by the Deutsche Forschungsgemeinschaft, Bonn, and the Fonds der Chemischen Industrie, Frankfurt.

References and Notes

(1) Lieser, G. *J. Polym. Sci., Polym. Phys. Ed.* **1983**, *21*, 1611.
(2) Geiss, R.; Volksen, W.; Tsay, J.; Economy, J. *J. Polym. Sci., Polym. Lett. Ed.* **1984**, *22*, 433.
(3) Yoon, D. Y.; Masciocchi, N.; Depero, L. E.; Viney, C.; Parrish, W. *Macromolecules* **1990**, *23*, 1793.
(4) Liu, J.; Geil, P. H. *J. Macromol. Sci., Phys.* **1992**, *B31*, 163.
(5) Economy, J.; Volksen, W.; Viney, C.; Geiss, R.; Siemens, R.; Karis, T. *Macromolecules* **1988**, *21*, 2777.
(6) Hanna, S.; Windle, A. H. *Polym. Commun.* **1988**, *29*, 236.
(7) Coulter, P. D.; Hanna, S.; Windle, A. H. *Liq. Cryst.* **1989**, *5*, 603.
(8) Kalika, D. S.; Yoon, D. Y. *Macromolecules* **1991**, *24*, 3404.
(9) Kalika, D. S.; Yoon, D. Y.; Iannelli, P.; Parrish, W. *Macromolecules* **1991**, *24*, 3413.
(10) Lukasheva, N. Y.; Sariban, A.; Mosell, T.; Brickmann, J. *Macromolecules* **1994**, *27*, 4726.
(11) van Ruiten, J.; Meier, R. J.; Hahn, C.; Mosell, T.; Sariban, A.; Brickmann, J. *Macromolecules* **1993**, *26*, 1555.
(12) Rutledge, G. C.; Suter, U. W. *Macromolecules* **1991**, *24*, 1921.
(13) Miazawa, T. *J. Polym. Sci.* **1961**, *55*, 215.
(14) Sugeta, H.; Miyazawa, T. *Biopolymers* **1967**, *5*, 673.
(15) Coulter, P.; Windle, A. H. *Macromolecules* **1989**, *22*, 1129.
(16) Jung, B.; Schürmann, B. L. *Macromolecules* **1989**, *22*, 477.
(17) (a) Lautenschläger, P.; Brickmann, J.; van Ruiten, J.; Meier, R. J. *Macromolecules* **1991**, *24*, 1284. (b) Jung, B.; Schürmann, B. *Macromolecules* **1992**, *25*, 1003. (c) Lautenschläger, P.; Brickmann, J.; van Ruiten, J.; Meier, R. J. *Macromolecules* **1992**, *25*, 1004.
(18) Jaffe, R. L.; Yoon, D. Y.; McLean, A. D. In *Computer Simulation of Polymers*; Roe, R. J., Ed.; Prentice-Hall: Englewood Cliffs, NJ, 1991; p 1.
(19) Coussens, B.; Pierloot, K.; Meier, R. J. *THEOCHEM* **1992**, *259*, 331.
(20) QCPE program No. 455. See also: Dewar, M. J. S.; Zoebisch, E. G.; Healy, E. F.; Stewart, J. J. P. *J. Am. Chem. Soc.* **1985**, *107*, 3902.
(21) Fabian, W. M. F. *J. Comput. Chem.* **1988**, *9*, 369.
(22) Fixman, M. *Proc. Natl. Acad. Sci. U.S.A.* **1974**, *71*, 3050.
(23) Dashevskij, V. G. *Conformazii* organitoheskih molecul; Khimia: Moscow, 1974; p 111.
(24) Block, H.; Walker, S. M. *Chem. Phys. Lett.* **1973**, *19*, 363.
(25) Sun, Z.; Cheng, H. M.; Blackwell, J. *Macromolecules* **1991**, *24*, 4162.
(26) Reiling, S.; Brickmann, J. *Macromol. Theory Simul.*, in press.

MA950234G